Single Crystal EPR Studies of $[enH_2][\{Fe(HEDTA)\}_2O]\cdot 6H_2O$ [en = Ethylenediamine; HEDTA = *N*-Hydroxyethylethylenediaminetriacetate(3−)]

Stephen J. W. Holgate,[1a] Gennadij Bondarenko,[1b] David Collison,*[,1a] and Frank E. Mabbs[1a]

Department of Chemistry, University of Manchester, Oxford Road, Manchester M13 MPL, UK, and Rostov State University, Rostov-on-Don, Russia

Received November 13, 1998

Single-crystal EPR studies of the Fe−O−Fe dimer, $[enH_2][\{Fe(HEDTA)\}_2O]\cdot 6H_2O$, have been performed at both X- and Q-band frequencies and room temperature. Resonances arising from the $S' = 1$, 2, and 3 states have been observed in the powder spectrum at Q-band frequency and analysis by spectral simulation has led to the zero-field splitting parameters: $|D_1| = 1.950\ cm^{-1}$, $|E_1| = 0.650\ cm^{-1}$, $|D_2| = 0.150\ cm^{-1}$, $|E_2| = 0.0195\ cm^{-1}$, $|D_3| = 0.570\ cm^{-1}$, and $|E_3| = 0.000\ cm^{-1}$. In addition, analysis of three orthogonal planes of single-crystal EPR data at both X- and Q-band frequencies has allowed the orientation of the zero-field splitting tensor with respect to the molecular geometry in the dominant ($S' = 2$) state to be determined. The largest principal value of the **D** tensor (D_{zz}) is found to lie approximately perpendicular to the plane of the Fe−O−Fe bridge; the nonlinear bridging angle is 165°. The results obtained in this study are compared with those from a number of other studies. A pattern for the orientations of the zero-field splitting parameters in the dominant spin state ($S' = 2$) of the Fe−O−Fe dimers, so far studied by single-crystal EPR spectroscopy, emerges.

Introduction

A large number of biologically and chemically significant molecules contains oxo-bridged polyiron centers. The reviews by Lippard[2] and Wilkins[3] include a number of examples of important polyiron-oxo proteins, including hemerythrin, ribonucleotide reductase, purple acid phosphatases, methane monooxygenase, and ferritin. An article by Hagen[4] covered some synthetic models of iron−oxygen aggregation and their possible relevance in biomineralization. A recent paper[5] by Powell et al. considered the syntheses, structures, and magnetic properties of Fe_2, Fe_{17}, and Fe_{19} oxo-bridged clusters and the possibility of them providing models for the biomineralization of iron.

Although iron oxo-bridged dimers have been studied extensively using magnetic susceptibility measurements,[6] there have been very few reports of EPR studies of such systems. A preliminary investigation was made by Okamura and Hoffman[7] of the title compound, $[enH_2][\{Fe(HEDTA)\}_2O]\cdot 6H_2O$.[8] EPR spectra of single crystals were observed at both X- and Q-band frequencies, and the main resonances in the spectra were assigned to the $S' = 2$ spin state. An X-band EPR study[9] has been reported of single crystals of $Na_4[\{Fe(EDTA)\}_2O]\cdot 12H_2O$ at various temperatures and crystal orientations. Variable temperature EPR spectra allowed the antiferromagnetic coupling constant, $J = -101\ cm^{-1}$, to be determined. Two types of lines were observed in the spectra. The first type, with stronger absorption intensity and sharper line widths, was assigned to the $S' = 2$ spin state, while broader lines with smaller absorption intensity attributed to the $S' = 1$ spin state appeared, mixed with the spectra of the $S' = 2$ spin state, at low temperatures, but had negligible intensity at room temperature. Analysis of the angular variation of the EPR spectra at room temperature, in planes perpendicular to each of the crystallographic axes (*a*, *b*, and *c*) in turn, led to values for the zero-field splitting parameters of $|D| = 0.21\ cm^{-1}$ and $|E| = 0.015\ cm^{-1}$. It was also found that the magnetic axes (*X*, *Y*, and *Z*) were related to the crystallographic axes to within a precision of 5°, by (*a*, *b*, *c*) = (*Y*, *Z*, *X*) for positive *E* (since the sign of *E* could not be determined, the *X* and *Y* axes are interchangeable). A study of binuclear iron(III) complexes of bipyridine (bpy) and phenanthroline (phen)[10] included the powder EPR spectra at X-band frequency of the complexes $[\{Fe(bpy)\}_2O][SO_4]_2\cdot 5H_2O$ and $[\{Fe(phen)\}_2O][SO_4]_2\cdot 6H_2O$. Magnetic susceptibility data led to values of the coupling constant, $J \sim -100\ cm^{-1}$, for both of the complexes. Although the EPR spectra showed quite a number of lines, no quantitative analysis was mentioned. It was simply reported that the decay of the EPR spectral intensity, as the temperature was lowered, indicated that the complexes were binuclear. It was also stated that the EPR spectra confirmed the fact that the ferric ions were in the high-spin state, since the temperature dependence of the spectra was consistent with the resonance lines originating from states with $S' = 1$. The powder EPR spectrum of $[\{Fe(Pc)\}_2O]$[11] has been reported to

* Corresponding author. Tel.: +44 161 275 4660/4653. Fax: +44 161 275 4598. E-mail: +david.collison@man.ac.uk.

(1) (a) The University of Manchester. (b) Rostov State University.
(2) Lippard, S. J. *Angew. Chem., Int. Ed. Engl.* **1988**, *27*, 344.
(3) Wilkins, R. G. *Chem. Soc. Rev.* **1992**, *21*, 171.
(4) Hagen, K. S. *Angew. Chem., Int. Ed. Engl.* **1992**, *31*, 1010.
(5) Powell, A. K.; Heath, S. L.; Gatteschi, D.; Pardi, L.; Sessoli, R.; Spina, G.; Del Giallo, F.; Pieralli, F. *J. Am. Chem. Soc.* **1995**, *117*, 2491.
(6) Kurtz, D. M. *Chem. Rev.* **1990**, *90*, 585.
(7) Okamura, M. Y.; Hoffman, B. M. *J. Chem. Phys.* **1969**, *51*, 3128.
(8) Abbreviations: EDTA, ethylenediaminetetraacetate(4−); en, ethylenediamine; HEDTA, *N*-hydroxyethylethylenediaminetriacetate(3−); bpy, 2,2′-bipyridyl; phen, 1,10-phenanthroline; Pc, phthalocyaninate(2−); salen, *N*,*N*′-bis(2-hydroxybenzyl)-1,2-ethanediamine(4−); Ssalen, *N*,*N*′-ethylenebis(thiosalicylideneiminato)(2−); *J* is defined by a Hamiltonian of the form $\mathbf{H} = -2J\ \hat{S}_1\cdot\hat{S}_2$.
(9) Esquivel, D. M. de S.; Ito, A. S.; Isotani, S. *J. Phys. Soc. Jpn.* **1976**, *40*, 947.
(10) Jezowska-Trzebiatowska, B.; Ozarowski, A.; Kozlowski, H.; Cukierda, T.; Hanuza, J. *J. Inorg. Nucl. Chem.* **1976**, *38*, 1447.
(11) Kennedy, B. J.; Murray, K. S.; Zwack, P. R.; Homburg, H.; Kalz, W. *Inorg. Chem.* **1985**, *24*, 3302.

10.1021/ic981317r CCC: $18.00
Published on Web 04/24/1999

have signals at $g \sim 6$ and $g \sim 2$. The signal at $g \sim 2$ appeared to consist of a well-resolved set of lines superimposed on a very broad line. The fine structure observed in the $g \sim 2$ region was explained as possibly arising from the antiferromagnetically coupled Fe(III)−O−Fe(III) moiety.

The magnetic moment of the complex $[\{Fe(Ssalen)\}_2O]\cdot py$ ($\mu_{eff} = 1.89\ \mu_B$ per Fe atom at 295 K)[12] was found to be similar to that of $[\{Fe(salen)\}_2O]$ ($\mu_{eff} = 1.87\ \mu_B$ per Fe atom at 300 K)[13] and other antiferromagnetically coupled binuclear μ-oxo-species in which each iron(III) center has $S = {}^5/_2$. However, the temperature dependence of the magnetic susceptibility of $[\{Fe(Ssalen)\}_2O]\cdot py$ was found to be quite different from that of $[\{Fe(salen)\}_2O]$ and indicated only weak interaction between the iron(III) ions. The EPR spectrum, in contrast to that of most other μ-oxo-species, was found to be characteristic of a rhombically distorted iron(III) ion with $S = {}^1/_2$. Nitrogen hyperfine splitting was observed on the central line of a spectrum in a pyridine glass.

Kurtz, in his review of oxo- and hydroxo-bridged diiron complexes,[6] stated that the problem in observing EPR signals in the oxo-bridged diferric system is that because the paramagnetic spin states are excited states, temperatures that significantly populate these states are likely to cause rapid relaxation of the electron spin, thus making the observation of EPR signals extremely difficult. Whether or not such signals are observable is also critically dependent on the magnitudes and signs of the zero-field splittings. Kurtz concluded by saying that, at the time the review was written, EPR spectroscopy could not be considered a reliable probe of the integer spin states arising from antiferromagnetic coupling in diiron complexes. Murray stated in his review of binuclear oxo-bridged iron(III) complexes[14] that there was clearly a need for more detailed EPR studies on such molecules.

A recent paper by Ozarowski et al.[15] contained the most complete analysis to date of EPR data for iron(III) oxo-bridged dimers. Single-crystal EPR studies were performed on two structurally characterized Fe−O−Fe dimers, $Na_4[\{Fe(edta)\}_2O]\cdot 3H_2O$ and $[\{Fe(phen)_2\}_2O][NO_3]_4\cdot 7H_2O$, for which the (antiferromagnetic) coupling constant, J, was -99 and $-110\ cm^{-1}$, respectively. The μ-oxo bridge angles in the two complexes are approximately 163° in the edta complex and 155° in the phen complex. Single-crystal EPR measurements were made at X-band frequency only. The crystals could not be oriented in the spectrometer using X-ray techniques, but for $Na_4[\{Fe(edta)\}_2O]\cdot 3H_2O$, the location of the crystal axes was fixed using the symmetry between the two magnetically inequivalent sites in the monoclinic space group. For each of the complexes, resonances attributable to the $S' = 2$ and $S' = 3$ states were observed. For the phen complex, a strong resonance appeared for certain orientations of the crystal but could not be confirmed as arising from the $S' = 1$ state. No resonances were observed for the $S' = 1$ state in the edta complex. A least-squares minimization method was used to obtain the spin-Hamiltonian parameters, D and E. The **g** matrix was assumed to be isotropic and equal to 2. A fit of the simulated angular variation of resonance positions to the experimental plot was reported for one plane of data only.

In this paper, the interpretation of the single-crystal EPR spectra of the iron(III) oxo-bridged dimer, $[enH_2][\{Fe(HEDTA)\}_2O]\cdot 6H_2O$, at both X- and Q-band frequencies and in three crystal planes, is reported. Magnetic susceptibility measurements[16] have yielded an antiferromagnetic coupling constant, $J = -95\ cm^{-1}$. The crystal structure of the compound has been reported[17] as monoclinic, space group $P2_1/c$ and the μ-oxo bridge angle is 165°.

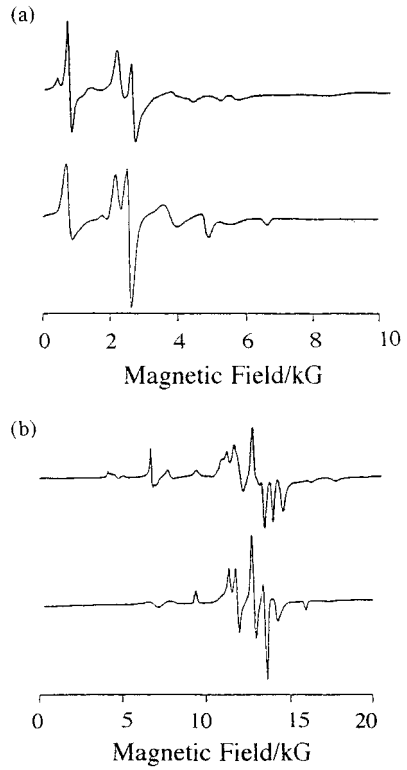

Figure 1. EPR spectra of powdered $[enH_2][\{Fe(HEDTA)\}_2O]\cdot 6H_2O$ at room temperature and (a) X-band frequency and (b) Q-band frequency. The upper spectrum in each case is the experimental spectrum and the lower is the spectrum simulated for the $S' = 2$ resonances.

Experimental Details.

Synthesis of $[enH_2][\{Fe(HEDTA)\}_2O]\cdot 6H_2O$. The compound was prepared as described in the literature.[18] Large, bright red, prismatic crystals were obtained by recrystallization from a dimethylformamide−water solution.

EPR Spectra. First-derivative EPR spectra were obtained on oriented single crystals of $[enH_2][\{Fe(HEDTA)\}_2O]\cdot 6H_2O$ at room temperature and both X- (ca. 9.25 GHz) and Q-band (ca. 35.0 GHz) frequencies (under nonsaturating conditions) with a Varian E112 spectrometer. The crystals were oriented such that spectra were obtained in the crystallographic *ca**, *ba**, and *cb* planes. EPR spectra of powdered samples of $[enH_2][\{Fe(HEDTA)\}_2O]\cdot 6H_2O$ were obtained at X-band frequency in the temperature range 300−77 K using the Varian E112 spectrometer with cooling of the samples being achieved using an Oxford Instruments ESR9 continuous flow cryostat. Q-band frequency EPR spectra of powdered samples were obtained using a Bruker ESP300E spectrometer, with temperatures in the range 300−100 K being obtained using a BVT2000 variable temperature unit, while for temperatures below 100 K, an ESR910 cryostat was used. Perpendicular detection mode was used at both of these frequencies. The use of parallel detection mode at X-band frequency on selected samples gave less well-resolved spectra, and so data collection with this mode was not continued. In

(12) Marini, P. J.; Murray, K. S.; West, B. O. *J. Chem. Soc., Chem. Commun.* **1981**, 726.
(13) Lewis, J.; Mabbs, F. E.; Richards, A. *J. Chem. Soc. A* **1967**, 1014.
(14) Murray, K. S. *Coord. Chem. Rev.* **1974**, *12*, 1.
(15) Ozarowski, A.; McGarvey, B. R.; Drake, J. E. *Inorg. Chem.* **1995**, *34*, 5558.
(16) Schugar, H. J.; Rossman, G. R.; Barraclough, C. G.; Gray, H. B. *J. Am. Chem. Soc.* **1972**, *94*, 2683.
(17) Lippard, S. J.; Schugar, H.; Walling, C. *Inorg. Chem.* **1967**, *6*, 1825.
(18) Schugar, H.; Walling, C.; Jones, R. B.; Gray, H. B. *J. Am. Chem. Soc.* **1967**, *89*, 3712.

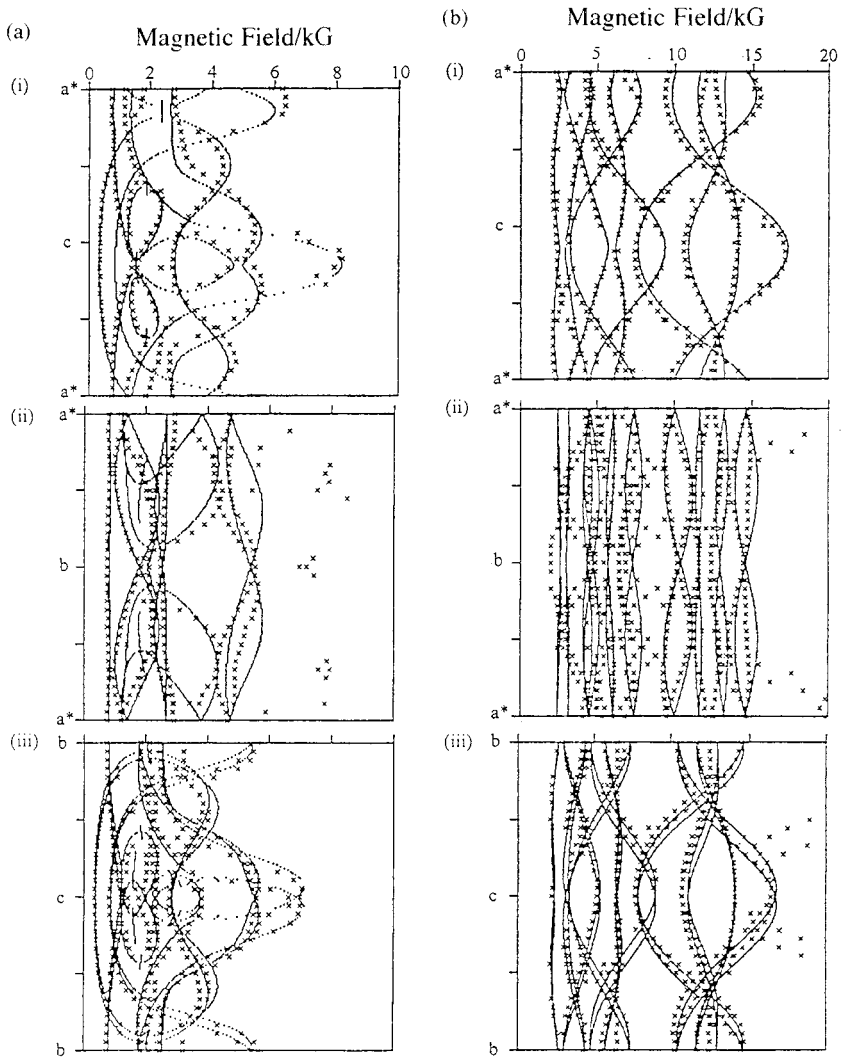

Figure 2. Experimental (×) and simulated (—) angular variation plots of resonance fields for the S′ = 2 state of $[enH_2][\{Fe(HEDTA)\}_2O]\cdot 6H_2O$ at room temperature and (a) X-band frequency and (b) Q-band frequency in the (i) *ca**, (ii) *ba**, and (iii) *cb* planes. The simulation parameters are in the text.

addition to the powder spectra measured in this laboratory, powder EPR spectra were recorded at W-band frequency (ca. 92.5 GHz) by Dr. Graham Smith at The University of St. Andrews, using a home-built spectrometer.

Results.

The EPR spectra of powdered samples of $[enH_2][\{Fe(HEDTA)\}_2O]\cdot 6H_2O$ at room temperature and X- and Q-band frequencies are shown in Figure 1. For a strongly antiferromagnetically coupled pair of iron(III) ions, each with $S = {}^5/_2$, there exists a set of six possible spin multiplets with S′ = 0, 1, 2, 3, 4, and 5, with S′ = 0 being the ground state. It has previously been shown[7] that the main features in the EPR spectra of this compound arise from the S′ = 2 state. Estimates of the spin-Hamiltonian parameters, *D* and *E*, for this spin state, were obtained by simulations of the powder spectra, using a method described previously[19] with *g* being assumed to be isotropic and equal to 2.00. The value of $|D|$ reported previously[7] was confirmed as being 0.15 cm^{-1} and in addition, a value of $|E|$ of 0.0195 cm^{-1} was determined. The simulations obtained are shown in Figure 1.

(19) (a) Collison, D.; Mabbs, F. E. *J. Chem. Soc., Dalton Trans.* **1982**, 1565. (b) Mabbs, F. E.; Collison, D. *Electron Paramagnetic Resonance of d Transition Metal Compounds;* Elsevier: Amsterdam, 1992; Chapter 16.

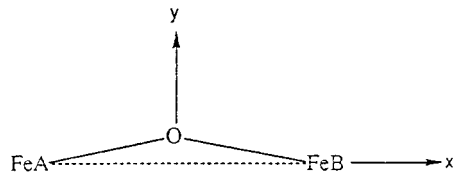

Figure 3. Location of the arbitrary molecular axes in $[enH_2][\{Fe(HEDTA)\}_2O]\cdot 6H_2O$. The *z* axis is perpendicular to the FeOFe plane.

The single-crystal EPR spectra at both X- and Q-band frequencies and room temperature were well-resolved. The angular variation plots of resonance positions for the three orthogonal planes of measurement are shown in Figure 2. To obtain simulations of these angular variation plots, it was necessary to modify the simulation procedure described previously.[19] In the original method, it was assumed that the principal axes of the **g** matrix and the zero-field splitting tensor were coincident with each other and with the molecular axes. However, in the present case, we needed to allow for noncoincidence of the zero-field splitting tensor axes and the molecular axes. This was done by setting up the molecular zero-field splitting tensor (using the values of *D* and *E* obtained from the best simulations of the powder spectra) with respect to a set of arbitrary molecular axes (*x*, *y*, *z*) as shown in Figure 3. The molecular axes were set up such that *x* lies along the FeA—

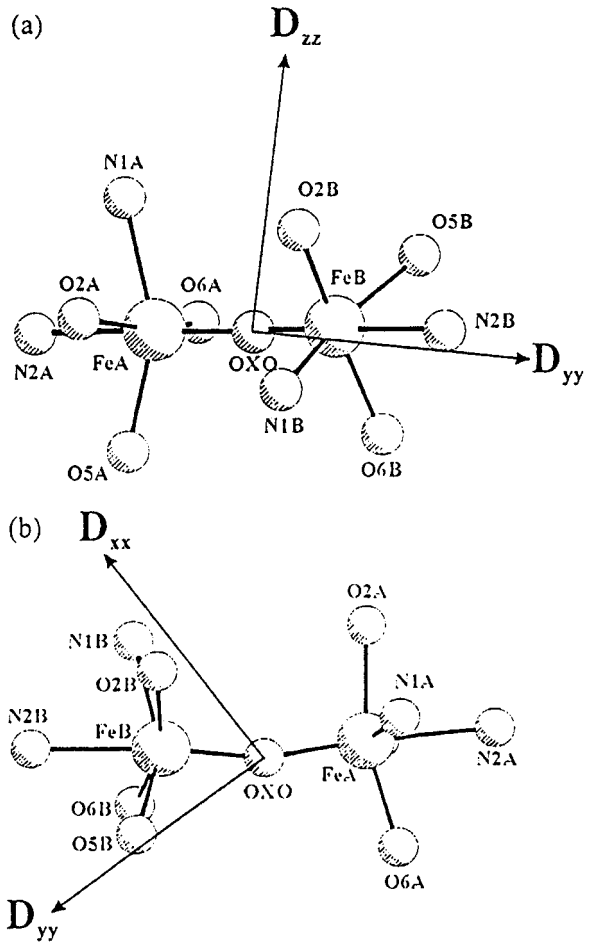

Figure 4. Relationship between the principal **D** tensor axes and the molecular structure of $[enH_2][\{Fe(HEDTA)\}_2O]\cdot 6H_2O$ viewed down the (a) D_{xx} axis and (b) D_{zz} axis.

FeB vector, *z* is the normal to the FeA−O−FeB plane, and *y* is the cross product of *z* and *x*. The molecular zero-field splitting tensor was transformed into the frame of reference with respect to which the single-crystal EPR spectra were measured. In general, it was found at this stage that there was a poor correspondence between the simulated and the experimental plots. Therefore, it was necessary to transform the zero-field splitting tensor away from the frame of measurement by using a set of Euler angles (α, χ, γ)[20] such that the best possible fits to the experimental spectra were obtained. The set of Euler angles was obtained by trial and error. The method relies upon obtaining optimal fits to the experimental data in three orthogonal planes. Further confirmation of the correctness of the Euler angles was provided by fitting data at more than one frequency. In the present case, in which no symmetry restrictions were imposed upon the zero-field splitting tensor, the set of Euler angles found to give the best fit to the data was $(\alpha, \chi, \gamma) = (30°, -20°, 30°)$. It was then possible to obtain the relationship between the principal axes of the zero-field splitting tensor and the molecular geometry. The results obtained in this way are schematically represented in Figure 4.

It is noted that in simulations of the angular variation at Q-band frequency, the simulations of the stronger, high-field resonances fit reasonably well to the experimental data, although the lower field features do not fit quite so well. The features unexplained by a simulation for the $S' = 2$ state may arise from other spin states. Some features were also observed in the Q-band powder spectrum which were not explained by the simulation for the $S' = 2$ state. Some of these unexplained features had line widths significantly narrower than those observed for the $S' = 2$ state and some, significantly larger line widths. This suggested that there may be contributions from the $S' = 1$ and $S' = 3$ states. The results of variable temperature powder EPR studies at X- and Q-band frequencies are presented in Figure 5. Beyond showing that a prominent feature in the Q-band powder spectrum at a magnetic field of approximately 6 kG disappears quite rapidly upon lowering the temperature, little useful information was obtained from this study. Estimates of the zero-field splitting parameters for the $S' = 1$ and $S' = 3$ states were made by simulation of powder spectra for these states for a variety of *D* and *E* values. The values found to give the best fits for the $S' = 1$ and $S' = 3$ states, respectively, were

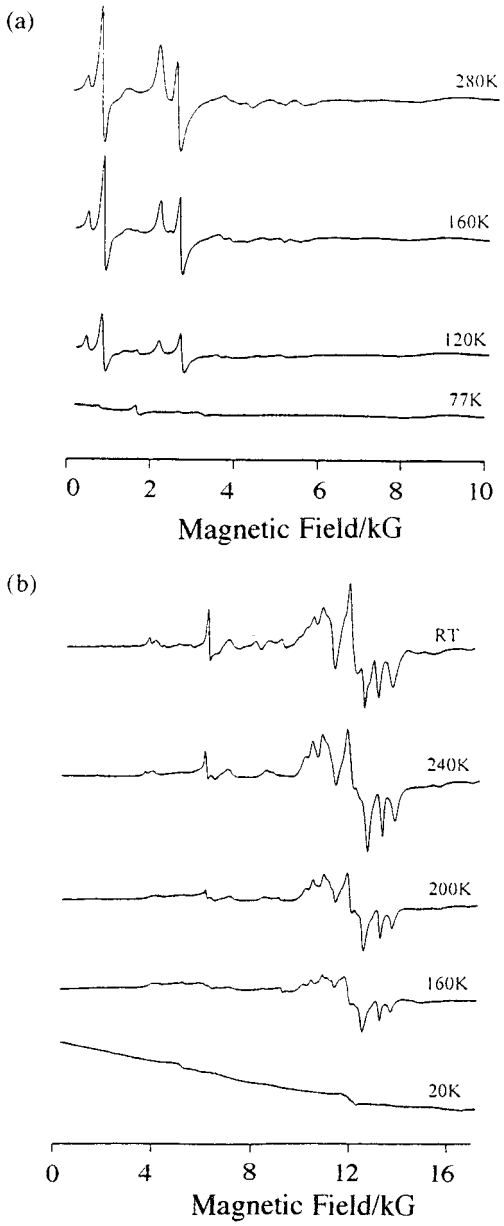

Figure 5. Variable temperature EPR spectra of $[enH_2][\{Fe(HEDTA)\}_2O]\cdot 6H_2O$ at (a) X-band frequency (9.250 GHz) and (b) Q-band frequency (34.200 GHz).

(20) The Euler angles are defined such that α is a rotation anticlockwise about the *z* axis, χ is a rotation anticlockwise about the new *x* axis, and γ is a rotation anticlockwise about the new *z* axis. See, for example: Mabbs, F. E.; Collison, D. *Electron Paramagnetic Resonance of d Transition Metal Compounds*, Elsevier: Amsterdam, 1992; Appendix 4.

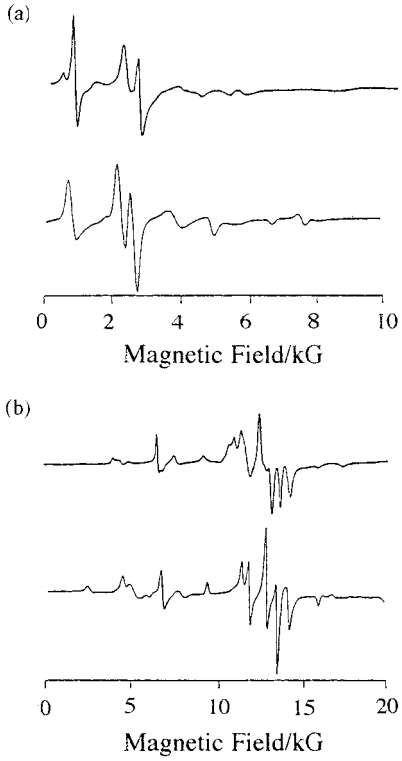

Figure 6. EPR spectra of powdered $[enH_2][\{Fe(HEDTA)\}_2O]\cdot 6H_2O$ at room temperature and (a) X-band frequency and (b) Q-band frequency. The upper spectrum in each case is the experimental spectrum and the lower is the spectrum simulated for the $S' = 1$, 2, and 3 resonances.

$|D_1| = 1.950\ cm^{-1}$, $|E_1| = 0.650\ cm^{-1}$ and $|D_3| = 0.570\ cm^{-1}$, $|E_3| = 0.000\ cm^{-1}$. The relative energies of the $S' = 0$, 1, 2, and 3 states for $[enH_2][\{Fe(HEDTA)\}_2O]\cdot 6H_2O$, calculated using the value of the coupling constant, $J = -95\ cm^{-1}$ [16] are 0, 190, 570, and 1140 cm^{-1}, respectively. The overall simulations of the powder spectra considering the $S' = 1$, 2, and 3 states were calculated assuming a Boltzmann population of these states. The simulations produced in this way are shown in Figure 6. It should be noted that the zero-field splitting parameters for the $S' = 1$ and $S' = 3$ states could not be determined with any great degree of certainty. Some of the resonances in the single-crystal spectra which are unexplained by a simulation for the $S' = 2$ state may well arise from the other spin states, but it was not possible to obtain fits for the data in these other states, due both to the paucity of resonances observed in these spin states and the fact that in the case of this compound, there are no symmetry restrictions placed upon the orientation of the zero-field splitting tensor.

In view of the large zero-field splitting for the $S' = 1$ state, it was thought that EPR spectra measured at a higher frequency than Q-band may yield some extra information concerning the spin-Hamiltonian parameters for this state. The powder EPR spectrum of $[enH_2][\{Fe(HEDTA)\}_2O]\cdot 6H_2O$ at W-band frequency (ca. 92.5 GHz) and 250 K is shown in Figure 7, together with a simulation using the best fit spin-Hamiltonian parameters from the simulations of powder spectra at X- and Q-band frequencies. Most of the features in the spectrum may be assigned to the $S' = 2$ state, and thus no further information concerning the $S' = 1$ level was obtained.

Discussion

The zero-field splitting parameters for $[enH_2][\{Fe(HEDTA)\}_2O]\cdot 6H_2O$ were estimated by simulation of the EPR powder spectra and were further refined by considering the single-crystal data. The axial zero-field splitting parameter for the $S' = 2$ state, $|D_2| = 0.150\ cm^{-1}$ confirmed the value reported previously.[7] In addition, the rhombic zero-field splitting parameter, $|E_2| = 0.0195\ cm^{-1}$, was determined. Additional resonances, not attributable to the $S' = 2$ level, some with much narrower line widths and some with much broader line widths, were observed in the powder spectrum at Q-band frequency. The resonances with narrower line widths were attributed to the $S' = 3$ state, and the zero-field splitting parameters, $|D_3| = 0.570\ cm^{-1}$ and $|E_3| = 0.000\ cm^{-1}$, were obtained. The resonances with much broader line widths were attributed to the $S' = 1$ state, although the parameters obtained for this state ($|D_1| = 1.950\ cm^{-1}$, $|E_1| = 0.650\ cm^{-1}$) were somewhat tenuous due to the paucity and broadness of these resonances.

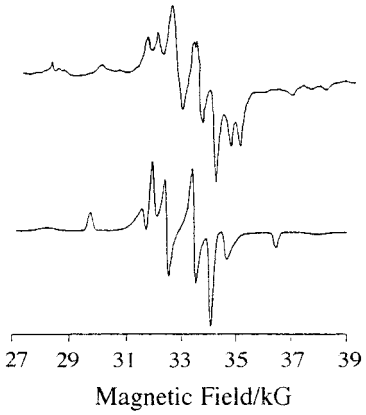

Figure 7. EPR spectra of powdered $[enH_2][\{Fe(HEDTA)\}_2O]\cdot 6H_2O$ at 250 K and W-band frequency ($\nu = 92.65$ GHz). The upper spectrum is the experimental spectrum and the lower is the spectrum simulated for the $S' = 2$ resonances.

Throughout the simulations in this study, an isotropic g value of 2.00 was used. This is a reasonable assumption for the present case, since the effect on the spectra of any small anisotropy in the **g** matrix is not nearly so great as anisotropy in the **D** tensor. In the present study, where a pure, undiluted compound was used, to be able directly to relate the spin-Hamiltonian parameters to the molecular structure, the effect of anisotropy in the **g** matrix is also masked by the broad line widths observed in the spectra. The introduction of a g-value anisotropy up to 0.05 g-value units did not lead to any significant variation in the simulated spectra.

For the $S' = 2$ state, the same spin-Hamiltonian parameters produced reasonable simulations of all the single-crystal EPR data at both X- and Q-band frequencies and the powder spectra at X-, Q-, and W-band frequencies. This gives us increased confidence in the correctness of these parameters.

To obtain reasonable fits of the simulated powder spectra to the experimental spectra, estimates had to be made of the line widths for the various spin states. The line widths were generally found to decrease with increasing value of S'. This may be a function of the population of the spin states. In other words, the higher spin states are effectively diluted by the lower states, although other mechanisms may be operative.[22]

The single-crystal EPR data were used to confirm the assignment of the spin-Hamiltonian parameters, obtained from the powder spectra, although in the single-crystal spectra of $[enH_2][\{Fe(HEDTA)\}_2O]\cdot 6H_2O$, it was generally only possible clearly to distinguish resonances arising from the $S' = 2$ level.

(21) This work.
(22) Smith, S. R. P.; Owen, J. *J. Phys. C.* **1971**, *4*, 1399.

Table 1. Spin-Hamiltonian Parameters[a] for Iron(III) Oxo-Bridged Dimers

compound	S'	$D_{S'}$	$E_{S'}$	ref
$Na_4[\{Fe(edta)\}_2O]\cdot 3H_2O$	1[b]	3.00	0.63	15
	2	0.248	0.06	15
	3	0.604	−0.016	15
$[\{Fe(phen)_2\}_2O][NO_3]_4\cdot 7H_2O$	1[b]	2.33	0.30	15
	2	0.256	0.037	15
	3	0.686	−0.008	15
$[enH_2][\{Fe(HEDTA)\}_2O]\cdot 6H_2O$	1[c]	1.95	0.64	21
	2	0.150	0.0195	21
	3[c]	0.57	0.000	21

[a] D and E are given in cm^{-1}. Their signs are relative, not absolute. [b] Calculated value. [c] Obtained by simulation of powder spectra.

Additionally, using the single-crystal data, it was possible to determine the orientation of the zero-field splitting tensor in relation to the molecular geometry. For the dominant $S' = 2$ state, the largest principal value of the zero-field splitting tensor (D_{zz}) was found to lie approximately perpendicular to the plane of the Fe−O−Fe bridge.

The zero-field splitting parameters obtained in this study are compared with those obtained for two other iron(III) oxo-bridged dimers in the recently published work of Ozarowski et al.[15] in Table 1. A similar trend in the values of D is observed for all three compounds. The magnitude of D in all three compounds is large, the dominant spin state for all the complexes ($S' = 2$) having values of $|D_2|$ in the range 0.15−0.35 cm^{-1} and the $S' = 3$ state yielding larger values, in the range $|D_3| = 0.45-0.70$ cm^{-1}. There does not appear to be as clear a pattern in the values of $E_{S'}$, although in general the values seem to be largest in the $S' = 1$ state and smallest in the $S' = 3$ state.

In the study by Ozarowski et al.,[15] the orientations of the principal axes of the zero-field splitting tensors with respect to the crystallographic axes in the $S' = 2$ and $S' = 3$ states only were determined for $Na_4[\{Fe(edta)\}_2O]\cdot 3H_2O$, while this information was not given for $[\{Fe(phen)_2\}_2O][NO_3]_4\cdot 7H_2O$. We have diagonalized the zero-field splitting tensors reported in ref 15 for $Na_4[\{Fe(edta)\}_2O]\cdot 3H_2O$ to yield the principal values and their direction cosines with respect to the crystallographic axes. It was then possible to relate the principal axes of the zero-field splitting tensor to the molecular structure. For the $S' = 2$ level, the largest principal value lies within approximately 15° of the normal to the Fe−O−Fe plane and for the $S' = 3$ level the largest principal value lies within 15° of the Fe−Fe vector. Thus, it appears that there may be a trend for the orientation of the zero-field splitting tensor in the $S' = 2$ state.

There were sufficient data from angular variation studies for the $S' = 3$ state of both compounds reported in ref 15 to allow all the individual elements of the **D** tensors for that state to be obtained, a situation not existing in the current study. The elements in combination with those of the $S' = 2$ states allowed those authors to estimate the principal values and the directions of the individual interaction tensors in their model, viz. point dipole $\mathbf{D}_{dip}$ and exchange $\mathbf{D}_{ex}$ (combined as $\mathbf{D}_e$) and local (single center) crystal field, $\mathbf{D}_c$, contributions. Using this treatment and following the work of Owen,[23] the overall **D** tensor for the $S' = 3$ state is determined primarily by the effect of $\mathbf{D}_e$, but those contributions may be comparable with that of $\mathbf{D}_c$ within the $S' = 2$ state. Whereupon, in the model used by Ozarowski et al.[15] the largest principal values of both the $\mathbf{D}_e$ and $\mathbf{D}_c$ tensors were deduced to lie close to the Fe−Fe vector for $Na_4[\{Fe(edta)\}_2O]\cdot 3H_2O$ and $[\{Fe(phen)_2\}_2O][NO_3]_4\cdot 7H_2O$, although the magnitude of the exchange contribution was found to be unexpectedly large.

A number of other studies of the electronic structure of oxo-bridged iron(III) dimers using other types of single-crystal spectroscopy have appeared in the literature. A paper by Schugar et al.[16] included the single-crystal electronic absorption spectra of $[enH_2][\{Fe(HEDTA)\}_2O]\cdot 6H_2O$. Among other conclusions, four intense UV absorption bands were assigned as being due to simultaneous-pair electronic (SPE) transitions, i.e. a single photon simultaneously exciting a ligand field transition on each ferric ion in the Fe−O−Fe unit. Single crystal electronic absorption spectroscopy revealed a broad band in the near-IR which was strongly polarized along the Fe−O−Fe direction. In the visible region of the spectrum, a band at 530 nm was found to be strongly polarized along the Fe−O−Fe direction. It was shown that a model featuring spin−spin coupling of high-spin iron(III) units could satisfactorily account for the electronic ground and excited-state properties of oxo-bridged iron(III) dimers. A more recent paper by Brown et al.[24] also included electronic structure studies of $[enH_2][\{Fe(HEDTA)\}_2O]\cdot 6H_2O$ using a number of techniques including single crystal, polarized, variable temperature electronic absorption, variable temperature magnetic circular dichroism (MCD), and variable temperature resonance Raman spectroscopies. A number of features were observed in the various spectra which were assigned as arising from the Fe−oxo−Fe dimer bond, and it was noted that this bonding dominates the absorption spectra of these species.

Although the other spectroscopic studies have highlighted the importance of the Fe−O−Fe linkage in determining the electronic structure of the iron(III) oxo-bridged dimer systems which have been used as models for various biomolecules such as hemerythrin and ferritin, the few single-crystal EPR studies to date have shown that in the dominant spin state ($S' = 2$) the largest principal axis of the zero-field splitting tensor does not, as might intuitively be expected, lie parallel to the Fe−O−Fe bridge, but lies perpendicular to it. The orientations of the zero-field splitting tensors in the other spin states (in particular $S' = 3$) show marked differences from that of the zero-field splitting tensor in the $S' = 2$ state. There is the potential for more information to be obtained from single-crystal EPR studies of these systems if higher magnetic fields are used, since such measurements may yield information regarding the large zero-field splittings predicted for the $S' = 1$ level and allow the various contributions to the zero-field splitting to be ascertained. It may also be expected that measurements at lower temperatures will aid in the assignment of the spectra arising from the $S' = 1$ level, although this does not appear to have been the case for the systems so far studied.

Acknowledgment. We thank The Royal Society (G.B. and D.C.) for financial support and the Duncan Campbell Fund at The University of Manchester for the provision of a studentship to S.J.W.H. Some of the work was carried out using the facilities of the EPSRC c.w. Multi-frequency EPR Service Centre at The University of Manchester. W-band EPR spectra were recorded by Dr. Graham Smith at The University of St. Andrews.

IC981317R

(23) Owen, J. *J. Appl. Phys.* **1961**, *32*, 213S

(24) Brown, C. A.; Remar, G. J.; Musselman, R. L.; Solomon, E. I. *Inorg. Chem.* **1995**, *34*, 688.